Polymer 50 (2009) 3403–3410

Contents lists available at ScienceDirect

Polymer

journal homepage: www.elsevier.com/locate/polymer

The phase behaviors of cylindrical diblock copolymers and rigid nanorods' mixtures

Linli He [a], Linxi Zhang [b,*], Hongping Chen [a], Haojun Liang [c]

[a] Department of Physics, Zhejiang University, Hangzhou 310027, PR China
[b] Department of Physics, Wenzhou University, Wenzhou 325027, PR China
[c] Department of Polymer Science and Engineering, University of Science and Technology of China, Hefei, Anhui 230026, PR China

ARTICLE INFO

Article history:
Received 13 February 2009
Received in revised form
12 April 2009
Accepted 29 April 2009
Available online 8 May 2009

Keywords:
Nanorod
Dissipative particle dynamics simulation
Morphology

ABSTRACT

Mixtures of cylindrical forming diblock copolymers (DBCPs) and mobile nanorods (NRs) are systematically investigated via dissipative particle dynamics (DPD) simulations. Final morphology of such composites depends not only on the characteristics of the copolymers, but also on the physical or chemical features of NRs, such as NR number, length, and surface adsorption (neutral, A and B attractive). A consideration of enthalpic and entropic interactions is necessary when physically or chemically distinct NRs are introduced into the copolymer/nanorod composites. For the short NRs, the phase behavior is similar to that of spherical nanoparticles (NPs). For the long NRs, the self-assembly of NRs can influence both the orientation and morphology of diblock/nanorod mixtures. If more NRs are incorporated, under stronger confinement from the host phase separated domains, the long NRs will aggregate and self-assemble into a certain spatial organization, inducing the morphological transitions of the composites from one phase to another. This behavior is not encountered for a similar system doped with spherical particles, emphasizing the role of particle shape in the interaction between doping particles and the host phase.

1. Introduction

The mixing of block copolymers (BCPs) and nanoparticles (NPs) has been practiced for decades, which possesses a variety of benefits over pure polymer systems. These advantages include increased strength, decreased gas permeability, improved heat resistance, and enhanced electrical conductivity [1–4]. With these superior properties, the polymer composites are suitable for electronic [5] and optoelectronic devices [6], magnetic storage [7], biomedical applications [8] and catalysis [9]. Therefore, such copolymer/particle composites have become an fundamental study and application in nanoscience and nanotechnology [10–14]. On the one hand, the microphase separation of the copolymers into nanoscopic, ordered domains could be harnessed to "template" the organization of the particles into nanoplanes, -wires, or -spheres within the polymer matrix [15,16], and thereby tailor the properties of the composites. For example, the optical performance of the composites is highly sensitive to the specific location of the particles within the matrix [17], and the extensive particle-filled domains can enhance the mechanical behavior of the entire system. On the other hand, the particles are not passive and can alter both the orientation [18,19] and the morphology [20–23] of the copolymers' microdomains. Hence, it is critically important to further understand how the presence of the particles affects the self-assembly of the copolymers and in turn, how the microphase separation of the polymer chains affects the phase behavior of the inclusions. Developing such an understanding is complicated by the fact that the number of parameters controlling the behavior of the system is large; the final morphologies of the mixtures will clearly depend on the size, shape, and concentration of particles, the composition of the copolymers, and the interaction energies between the different species.

In the last decades, many experiment [23–26], theory [15,16,20,27] and simulation [28–30] studies mainly focused on the mixtures of DBCPs and spherical NPs. Experimentally, Yeh et al. reported that CdS NPs, segregated into the P4VP domains of S4VP block copolymers, induced the morphological change of the CdS/S4VP composites from hexagonally packed P4VP cylinders to lamellar, and finally to disordered structures [23]. Thompson et al. combined self-consistent field (SCF) and density functional theories (DFTs) to investigate the mesoscopical phase behavior of diblock copolymers'/spherical NPs' mixtures. The phase diagrams as a function of the block composition f and the particle relative parameters, such as the size, concentration and surface adsorption, have been obtained [15,16]. Their results indicate that in such complex mixtures, the ordering of the copolymers templates the spatial organization of the particles [15,16], meanwhile, the

* Corresponding author. Tel.: +86 571 87952133; fax: +86 571 87951328.
E-mail address: lxzhang@zju.edu.cn (L. Zhang).

0032-3861/$ – see front matter © 2009 Elsevier Ltd. All rights reserved.
doi:10.1016/j.polymer.2009.04.068

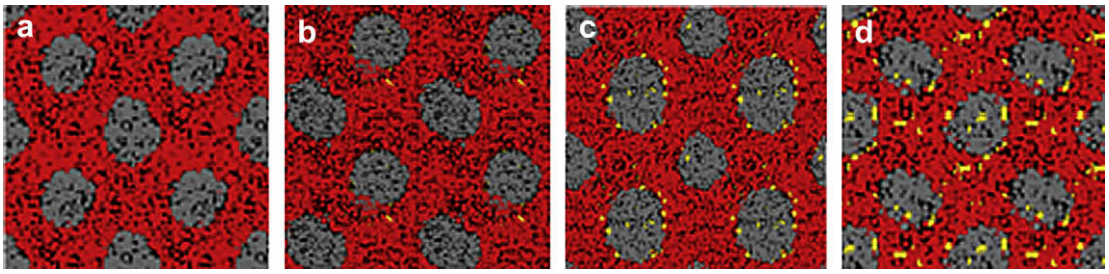

Fig. 1. Morphologies of DBCPs and neutral NRs' mixtures for $N_{rod} = 0$ (a), 30 (b), 70 (c) and 160 (d), with $L_{rod} = 0.3$. A and B blocks are presented in gray and red, and the NRs are shown in yellow, respectively. (For interpretation of the references to colour in this figure legend, the reader is referred to the web version of this article.)

particles can in turn affect the self-assembly of the polymer chains [20,27]. Huh et al. presented simulation results that by varying the particle size and concentration, one can modify the morphology of the resulting mixtures and either induce macroscopic phase separation between the particle-rich and diblock-rich phases or create potentially new microphase-separated structures [28].

It is well established that the phase behavior of anisotropic NPs is different from that of spherical NPs, due to the effect of the additional orientational entropy resulting from the particles' anisotropy. The situation for the copolymer/particle mixtures becomes much more complex if dispersed NPs are in high-aspect-ratio, such as nanorods (NRs), because the NRs can form liquid crystalline phases [31]. The high-aspect-ratio particles will result in polymer nanocomposites processing superior optical and mechanical properties relative to polymers reinforced with an equivalent volume fraction of spherical particles [32]. In recent work, Huyne et al. blended inorganic NRs and polymers to fabricate solar cells that possesses greater efficiencies than conventional organic photovoltaic cells, since the long axis of the rod provides a continuous channel for transporting electrons, an advantage over spherical particles where electron hopping between particles will be required [33]. Peng et al. showed that immersing NRs into a binary phase-separating blend could drive the NRs to form percolating networks at relatively low volume fractions. These extensive networks can potentially improve both the mechanical and electrical properties of the copolymer/nanorod mixtures [10].

Recently, there are increasing interests in the studies of the mixtures which consist of copolymers and immobile [34–37] or mobile [38–45] NRs. Laicer et al. investigated the mixture of cylindrical forming DBCPs and immobile NRs using experimental and computational methods. They illustrated a general mechanism for the kinetic templating of copolymer domains from NR seeds [34,35]. In our recent work, we used the SCF theory to study the self-assembly of symmetric DBCPs' films with embedded one or two NRs. We found that with appropriate NR size and interaction strength, the NRs not only could promote the formation of incomplete cylindrical and spherical structures near the film surfaces, but also induce complete lamellar, cylindrical and spherical structures in the interior of the thin film [37]. In addition, Zhang et al. described the assembly of mobile CdSe NRs in diblock copolymer templates, PS-b-PMMA, one with lamellar nanoscopic channels and the other with cylindrical nanoscopic pores. By choosing an appropriate NR dimensions relative to the channel or pore width, they can control the orientation and lateral position of NRs. For the former, the NRs have the tendency to align along the lamellar channel. For the latter, each of the cylindrical pores contains several no preferred orientation of NRs, due to the symmetry of the pore cross-section [38]. Bećneut et al. experimentally investigated magnetic NRs confined in a lamellar lyotropic phase. They also found that when the NRs were oriented, the texture of the lamellar phase changed accordingly. In addition, the lamellar phase induced an attractive interaction between the NRs [39].

The cooperative interactions between mesophase-forming copolymers and NRs can yield well-ordered hybrid materials. However, besides above experimental researches [38–41] recent theory [10] and simulation [42–44] studies mainly focus on the two cases: the copolymers embedded with immobile NRs and binary

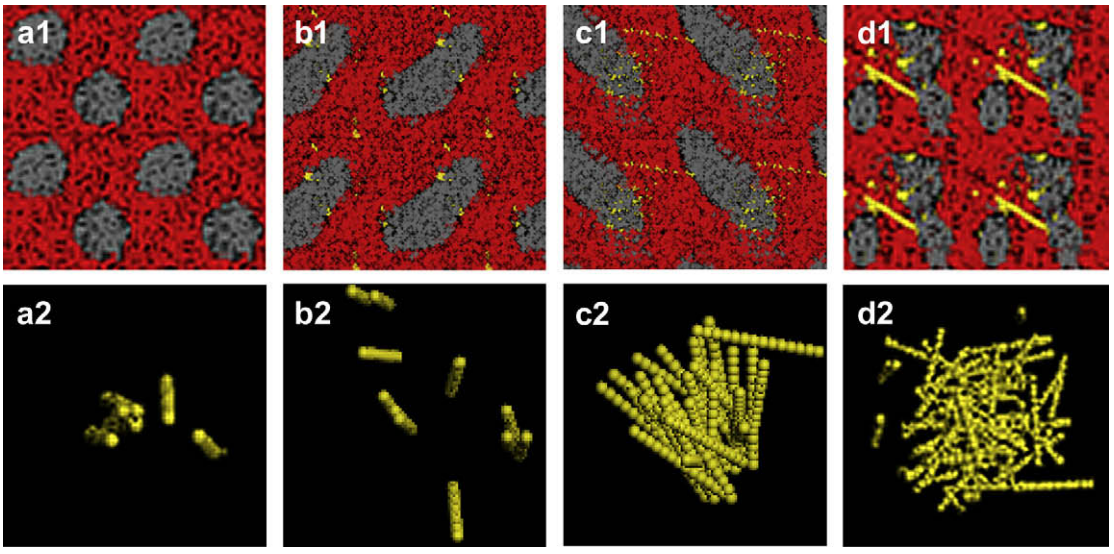

Fig. 2. Morphologies and NRs' distributions of DBCPs and neutral NRs mixture for $N_{rod} = 6$ (a1–a2), 10 (b1–b2), 30 (c1–c2) and 80 (d1–d2), with $L_{rod} = 3.9$.

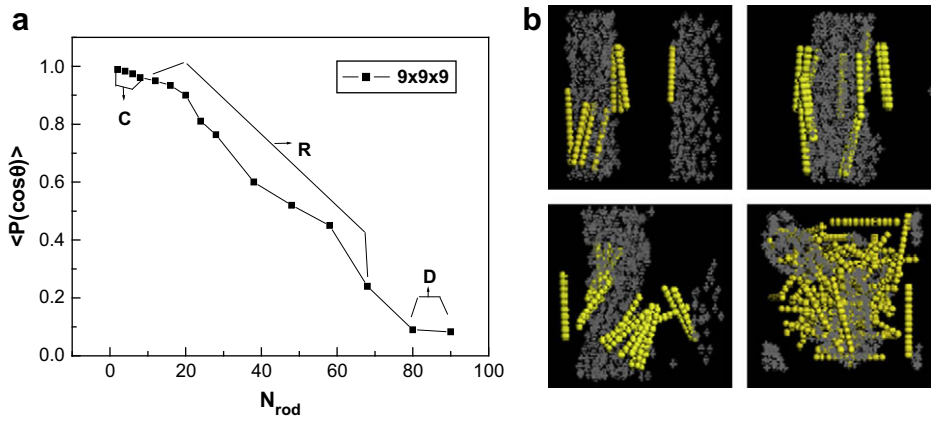

Fig. 3. (a) Average NRs' orientation $\langle P(\cos\theta)\rangle$ as a function of NR number N_{rod} for DBCPs and neutral NRs' mixtures with $L_{rod} = 3.9$. (b) The NRs' spatial distribution and positional orientation in the diblock matrix with $N_{rod} = 8$, 16, 28 and 80. Only A blocks and NRs are shown.

mixtures containing mobile NRs. The investigations about the mixtures of a kind of DBCPs and mobile NRs with concerning different NR parameters, such as NR number, length, and surface adsorption, are comparatively few. Nevertheless, the controlling of these parameters in the practical application is of great significance. As well known, the final structures of copolymer/particle composites depend not only on the features of the particles but also on the characteristics of the copolymer. To readily compare with our previous work [45], which focuses on the mixtures of symmetric A_5B_5 ($f_a = 0.5$) and A-attractive rigid NRs, here, we use the same parameters and the only value we change is the diblock composition parameter: $f_a = 0.3$. In this report, we extend the dissipative particle dynamics (DPD) method to deal with the NRs dispersed in cylindrical diblock copolymer melts. By introducing a serial of parameters, such as NR number, length, and surface adsorption, we substantially analyse the phase behaviors and novel morphologies of the hybrids. Some results are in qualitative agreement with recent experimental studies [38,39], and can also provide new guidelines for creating materials with new morphologies and functions.

2. Theory and model

In 1992, Hoogerbrugge and Koelman [46] proposed a new simulation technique referred to as dissipative particle dynamics (DPD), appropriate for the investigation of the generic properties of macromolecular systems. Within the DPD approach [46,47] fluid particles are coarse grained into 'beads' or DPD particles, which interact with each other via conservative, dissipative, and random forces.

$$\vec{F}_{ij}^{C} = a_{ij}\omega(r_{ij})\hat{r}_{ij} \tag{1}$$

$$\vec{F}_{ij}^{D} = -\gamma\omega^2(r_{ij})\left(\hat{r}_{ij}\cdot\vec{v}_{ij}\right)\hat{r}_{ij} \tag{2}$$

$$\vec{F}_{ij}^{R} = \sigma(\Delta t)^{-1/2}\omega(r_{ij})\xi_{ij}\hat{r}_{ij} \tag{3}$$

where $\vec{r}_{ij} = \vec{r}_i - \vec{r}_j$, $r_{ij} = |\vec{r}_{ij}|$, $\hat{r}_{ij} = \vec{r}_{ij}/r_{ij}$, and $\vec{v}_{ij} = \vec{v}_i - \vec{v}_j$. $\omega(r)$ is a weight function, for which we adopt the commonly used form

$$\omega(r) = \begin{cases} 1 - r/r_C & r_{ij} \le r_c \\ 0 & r_{ij} > r_c \end{cases} \tag{4}$$

The strength of the conservative force is governed by the positive constant a_{ij}. ξ_{ij} is a symmetric random variable with zero mean and unit variance, and is uncorrelated for different times and different particle pairs.

The combination of the dissipative and random forces constitutes a thermostat. The fluctuation–dissipation theorem requires that σ and the friction parameter γ are related through the relation

$$\sigma^2 = 2\gamma k_B T \tag{5}$$

where k_B is Boltzmann's constant. For convenience, the cutoff radius r_c, the energy k_BT and the particle mass m are all taken as unity. Here, $\gamma = 6.57$ and the temperature $k_BT = 1$. Therefore, $\sigma = 3.62$ according to Eq. (5).

Additionally, for the polymers, the spring force $\vec{f}_i^{S}$, which acts between the connected beads in a chain, has the form of

$$\vec{f}_i^{S} = \sum_j C\vec{r}_{ij} \tag{6}$$

where C is a harmonic type spring constant for the connecting pairs of beads in a polymer chain, chosen to be equal to 4 here (in terms of k_BT) [48].

According to the approach taken by previous studies [49–51] in the DPD simulation, solid particles also can be constructed from some DPD beads. Similarly, in this report, the rigid NR is composed of a number of DPD particles N_p, with a fixed distance D_{p-p} between consecutive particles, so that corresponding length of an NR is defined as $L_{rod} = (N_p - 1) \times D_{p-p}$ [49]. In order to avoid undesired

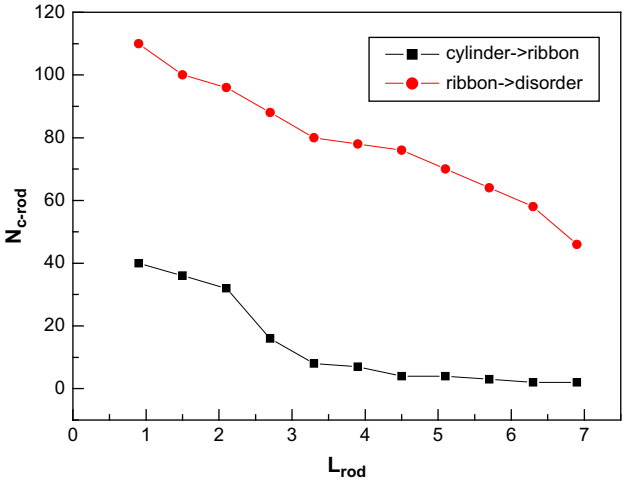

Fig. 4. The critical nanorod number $N_{c\text{-}rod}$ as a function of the nanorod length L_{rod} for DBCPs and neutral NRs' mixtures. Here, L_{rod} varies from 0.9 to 6.9.

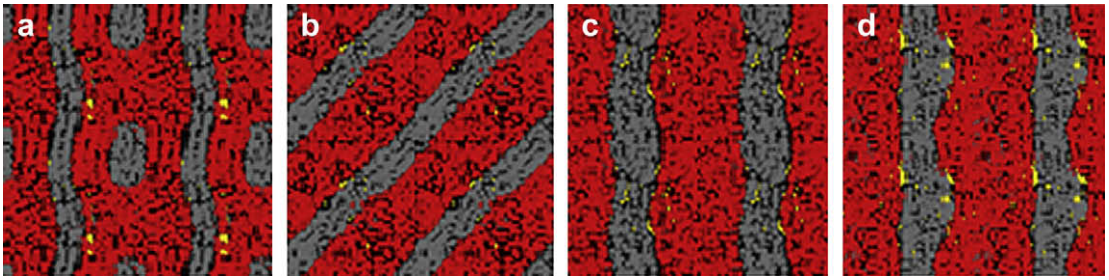

Fig. 5. Special morphologies of DBCPs and neutral NRs' mixtures for $L_{rod} = 44$ with $L_{rod} = 3.3$ (a), $N_{rod} = 36$ with $L_{rod} = 4.5$ (b), $N_{rod} = 30$ with $L_{rod} = 5.1$ (c) and $N_{rod} = 60$ with $L_{rod} = 5.7$ (d).

penetration of fluid particles into the NRs, and overlap between NRs, the number density of the DPD particles in an NR is larger than the number densities of the A or B block. Here, D_{p-p} is fixed at 0.3 and the range of NR length is 0.3–6.9. Meanwhile, we also calculate the radius gyration of free polymers (A_3B_7) $\langle S^2\rangle^{1/2} = 2.2$ and the corresponding cylindrical pores diameter $D = 3.0$, respectively. Therefore, the range of the ratio of L_{rod}/D is about from 0.1 to 2.3, which is very close to the experiment results of $L_{rod}/D = 0.7$–2.0 [38].

All DPD particles interact with each other via the same conservative, dissipative, and random forces, according to Eqs. (1)–(3). For the fluids, the Newton equations for particles' positions and velocities are solved by a modified version of the velocity Verlet algorithm [52]. Then for the NRs, a constraining routine is used to keep the inner particles aligned and equidistant during the simulation. In short, the forces on the DPD particles of an NR are converted into a net force on the two end DPD particles, and the equations of motion for these two DPD particles are solved, using the standard shake routine to keep them at a fixed distance. The positions of the $N_p - 2$ intermediate DPD particles are then readily calculated by a linear interpolation at the end of each time-step [49].

At first, we use this compiled DPD program to investigate the bulk morphologies for pure A_3B_7, and the results are consistent with the commercial software (Material Studio, Accelrys Software Inc, USA) and previous study [52]. Our model system consists of the mixtures of the cylindrical forming DBCPs (A_3B_7) and mobile NRs. The interaction parameters of the mesoscopic model are estimated by performing lower scale (i.e., atomistic molecular dynamics (MD)) simulations, and the relationship between the repulsion parameter and the density in a real polymeric system has been provided in previous studies [49,53,54]. The amplitudes, a_{ij}, of the conservative forces between the three types of DPD particles (A, B, and N), are given by $a_{AA} = a_{BB} = 15$, $a_{AB} = 30$, $a_{NN} = 15$, and the variable $a_{A(B)N}$. In this study, three types of NRs are considered: (a) neutral, which have no preference to either of diblock ($a_{AN} = a_{BN} = 20$); (b) A-attractive, which energetically prefers the A blocks ($a_{AN} = 15$ and $a_{BN} = 20$); (c) B-attractive, which energetically prefers the B blocks ($a_{AN} = 20$ and $a_{BN} = 5$). Because the NRs tend to aggregate within polymers, this choice of repulsive interaction a_{NN} can avoid the overlap between NRs to some extent. Initially, fluid particles are arranged in a face-centered-cubic (fcc) lattice via spring forces, and the mobile NRs are randomly dispersed in the fluids. Periodic boundary conditions are applied in all three directions.

3. Results and discussion

According to the previous researches [36,38–40], it is indicated clearly that for copolymer/nanorod mixtures, we should comprehensively study: (i) the guidance of NRs to the self-assembly of copolymers [36], and (ii) the influence of the confinement from the copolymer matrix on the phase behavior of NRs [38–40]. In this report, we consider three types of NRs (neutral, A and B attractive), to analyse the cooperatively induced phase behaviors and morphologies of the mixtures in detail.

3.1. Neutral nanorods

Here, we perform the DPD simulation on the self-assembly of A_3B_7 and neutral NRs' mixtures. Because of the limitation of the computer, the size of system used in our calculation is much smaller than that in experiment. To eliminate the size effect in simulation, we use the same method [45] to calculate the bulk characteristic periods L_0 for different size systems, and finally focus on the $9 \times 9 \times 9$ DPD units' system, containing 3645 DPD fluid particles for the density of $\rho = 5$. In order to observe the complete periodic structures, the morphologies of the mixtures presented in the following figures are composed of four replicated $9 \times 9 \times 9$ DPD units snapshots. Fig. 1(a) shows the cylindrical phase of pure A_3B_7, which is consistent with the previous study [52]. We first consider the case of short NRs with $L_{rod} = 0.3$ in Fig. 1(b)–(d), corresponding to $N_{rod} = 30$, 70 and 160, here N_{rod} represents the NR number. According to Fig. 1, it can be clearly seen that the phase behavior of NRs is similar to that of spherical NPs [15,27,55]. The NRs mainly are located at the interface between A and B blocks, and the mixtures preserve cylindrical structure (*C*), because the stretching required by the BDCPs to circumvent the solid NRs is less significant. Under this condition, the melt of copolymers can affect the phase behavior

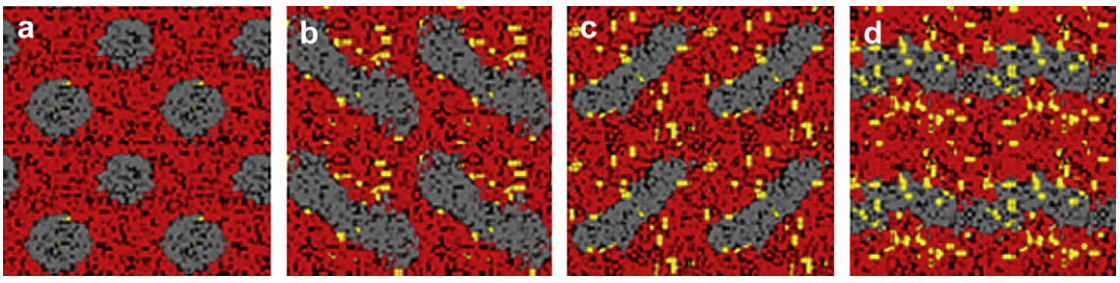

Fig. 6. Morphologies of DBCPs and A-attractive NRs' mixtures for $N_{rod} = 20$ (a), 120 (b), 200 (c) and 300 (d), with $L_{rod} = 0.3$.

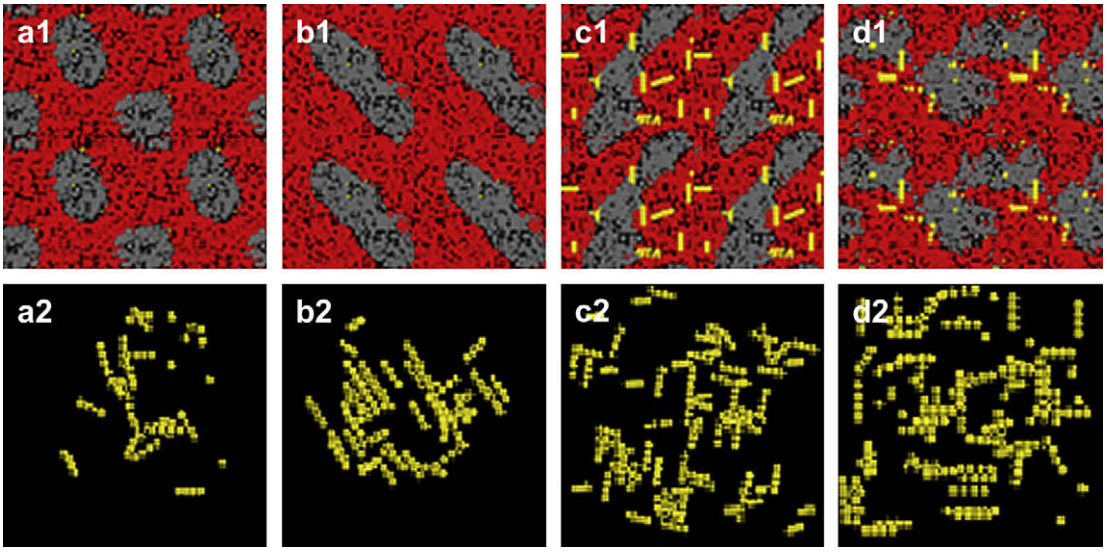

Fig. 7. Morphologies and NRs' distributions of DBCPs and A-attractive NRs' mixtures for $N_{rod} = 30$ (a1–a2), 48 (b1–b2), 76 (c1–c2) and 84 (d1–d2), with $L_{rod} = 0.9$.

of NRs and direct its spatial organization, but the neutral short NRs almost has no effect on the morphology of copolymers. Then, for cases of varying L_{rod} from 0.6 to 6.9, with the increase of N_{rod}, we find that the morphologies of the mixtures for different L_{rod} all undergo a similar transition. The corresponding morphological transition of the mixtures can be expressed as C → R → D, where C, R and D respectively represent the structures of cylinder, ribbon and disorder. Here, take $L_{rod} = 3.9$ for example, in order to study deeply the phase behavior of NRs in the polymer matrix, we also present the NRs' distribution of one $9 \times 9 \times 9$ DPD units' period in Fig. 2(a2)–(d2). In Fig. 2, the three structures of cylinder (C), ribbon (R) and disorder (D) are observed, corresponding to $N_{rod} = 6$, $N_{rod} = 10$, 30, and $N_{rod} = 80$. Substantially, the forming of these series of morphologies (C, R and D) mainly depends on the competition of the interface confinement from the host phase and the collective phase behaviors of NRs (the interactions and anisotropy). Therefore, it can be easily understood that when N_{rod} is small, due to the strong interface confinement, the mixtures preserve the cylindrical phase (C) with NRs distributed in the interface and oriented along the direction of cylindrical pore; when N_{rod} exceeds a certain extent, the interactions between NRs mainly account for the morphology of the hybrids, so the disordered structure (D) with NRs oriented randomly in the fluid not only in the interface of diblock is observed in Fig. 2(d1)–(d2); the intermediate case, the ribbon structure (R), shown in Fig. 2(b1)–(c1), is cooperatively induced by the interface confinement and the collective phase behaviors of NRs (the interactions and anisotropy).

Due to the NRs' shape anisotropy, the orientation of NRs becomes highly sensitive to the host phase domains. In order to present clearly the positional orientation of NRs within the diblock mixtures, we define the angle of NRs' orientation with respect to the certain direction (i.e., z axis) as θ. In fact, the direction of cylindrical pore is basically along z axis. Then, we calculate the average NRs' orientation relative to the z axis within the polymers' matrix as follow:

$$\langle P(\cos\theta)\rangle = \left\langle \left(3\cos^2\theta - 1\right)/2 \right\rangle \tag{7}$$

$\langle P(\cos\theta)\rangle$ will take values of −0.5, 0, and 1 for NRs that are perpendicular, randomly oriented and parallel to the z axis [45].

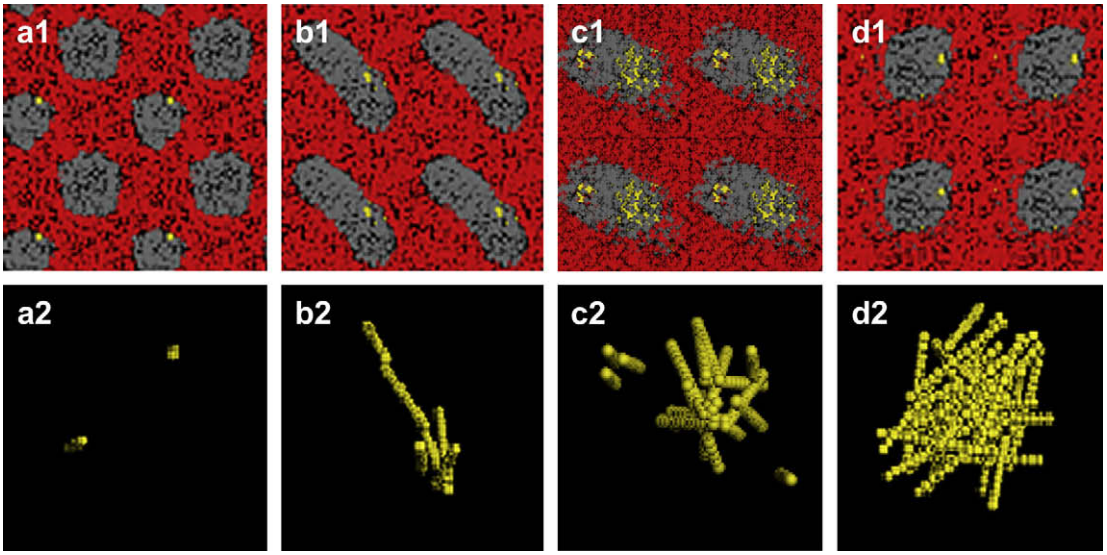

Fig. 8. Morphologies and NRs' distributions of DBCPs and A-attractive NRs' mixtures for $N_{rod} = 2$ (a1–a2), 6 (b1–b2), 20 (c1–c2) and 36 (d1–d2), with $L_{rod} = 3.9$.

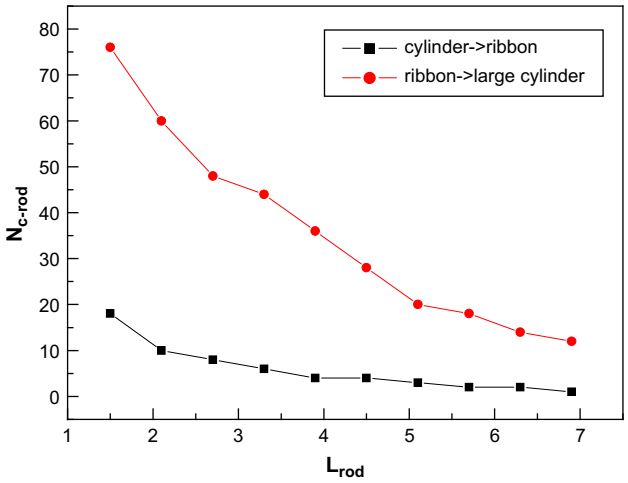

Fig. 9. The critical nanorod number $N_{c\text{-}rod}$ as a function of the nanorod length L_{rod} for DBCPs' and A-attractive NRs' mixtures. Here, L_{rod} varies from 1.5 to 6.9.

Fig. 3(a) shows the average NRs orientation $\langle P(\cos\theta)\rangle$ as a function of NR number N_{rod}, and corresponding morphologies of copolymer/nanorod mixtures. For the cylindrical phase (C), the values of $\langle P(\cos\theta)\rangle$ are close to 1.0, indicating that the NRs' long axis is basically along the direction of cylindrical pore. Contrarily, for the disordered structure (D), the values of $\langle P(\cos\theta)\rangle$ are close to 0, meaning that the NRs are oriented randomly in the host fluids. For the ribbon structure (R), according to Fig. 3(a), the values of $\langle P(\cos\theta)\rangle$ decrease as the increase of N_{rod}, the orientation of NRs becomes more and more dispersed, and finally cause the formation of disordered structure (D). Correspondingly, Fig. 3(b) presents the NRs' spatial distribution and positional orientation at the interface of diblock, qualitatively.

To visualize the effects of NR length L_{rod} on the self-assembled structures of diblock/nanorod mixtures, we calculate the critical NR number $N_{c\text{-}rod}$ as a function of L_{rod} in Fig. 4. The squares and circles respectively represent the critical NR number $N_{c\text{-}rod}$ for the mixtures transiting from cylinder to ribbon and from ribbon to disorder. From Fig. 4, it is clear that the longer the NR length L_{rod} is, the stronger the effect on the final morphology is, that is, the easier causing morphological transition is. In addition, surprisingly, in specific L_{rod} and N_{rod}, some special ordered structures for DBCPs and neutral NRs mixtures, such as cylindrical-lamellar (C–L) and complete lamellar (L) structures, are observed in Fig. 5(a) and Fig. 5(b)–(d), which can be regarded as intermediate states during the morphological transition.

3.2. A-attractive nanorods

In this section, we investigate the morphologies for cylindrical DBCPs embedded with A-attractive NRs. Fig. 6 shows the case of short NRs with $L_{rod} = 0.3$, corresponding morphological transition expressed as C → R → L. It can be inferred that the incorporation of A-attractive NRs equivalently improve the A-block composition (f_a), giving rise to a phase transition from cylindrical to lamellar structure, whose behavior is similar to that of spherical NPs [23]. Furthermore, it also indicates that the effects of the shape anisotropy of NRs have not been represented. However, due to the NRs preferentially wetted by the minor component (A) of diblock, the self-assembly of the mixtures becomes so sensitive to L_{rod} that the morphological transition of the system shows different regularities as the increase of L_{rod}. With a little increase in L_{rod}, the mixtures follow a transition as C → R → D, corresponding to $L_{rod} = 0.9$ in Fig. 7. Nevertheless, when we increase L_{rod} from 1.5 to 6.9, the mixtures follow another transition as C → R → C′, corresponding to $L_{rod} = 3.9$ in Fig. 8. Here, C′ represents the large cylindrical structure, whose cylindrical repeat distance is higher than that of the bulk cylindrical phase (C). According to above inference in Section 3.1, these series morphologies (C, R, D and C′) are formed by the competition of the interface confinement from the host phase and the collective phase behavior of anisotropic NRs. Comparing with the two cases of $L_{rod} = 0.9$ and $L_{rod} = 3.9$, we find that when more NRs are added into the fluid, the final morphologies of the mixtures appear as disordered (D) and large cylindrical (L_{rod}) structures, respectively. It can be further understood as follow: with more NRs incorporated, the long NRs under stronger confinement from A phase domains will form aggregates, inducing a transition from ribbon (R) to large cylindrical structure (C′), whereas the short NRs are not.

Essentially, the competition of the interface confinement and the collective phase behavior of anisotropic NRs can be rationalized on the basis of considering the relative enthalpic and entropic effects involving all of the species, A, B blocks and NRs. On the one hand, the NRs' distributions reveal a degree of enthalpically driven self-assembly, due to the interactions among species. On the other hand, the NRs' aggregates and orientation show a degree of entropically generated self-assembly, based on the inherent shape anisotropy of NRs and confinement of narrow phase separated domains. Recently, Bećneut et al. experimentally observed the similar results for lamellar diblock and magnetic NRs mixtures: the orientation of NRs determines the texture of the lamellar phase; on the other hand, the lamellar phase induces an attractive interaction between the NRs. In more concentrated lamellar phases (under stronger confinement), the NRs form aggregates [39]. Additionally, Huh et al. used Monte Carlo simulations to investigate the mixtures of cylindrical diblock and spherical NPs. They found that when the particle volume fraction was low, the mixtures were in the cylindrical phase, with the NPs randomly dispersed within the A cylinders; as the particle volume fraction was increased, the NPs segregated from the diblocks and self-assembled into a "core" cylinder, surrounded by a "shell" consisting of the A-block. As a result, the system exhibited the apparent two-phase coexistence between the pure diblock and some "mixed" phase in which particles and diblocks were microphase-separated [28].

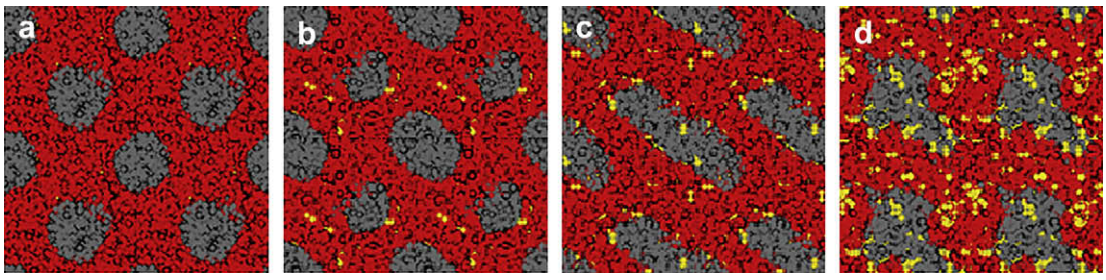

Fig. 10. Morphologies of DBCPs' and B-attractive NRs' mixtures for $N_{rod} = 8$ (a), 28 (b), 52 (c) and 100 (d), with $L_{rod} = 0.3$.

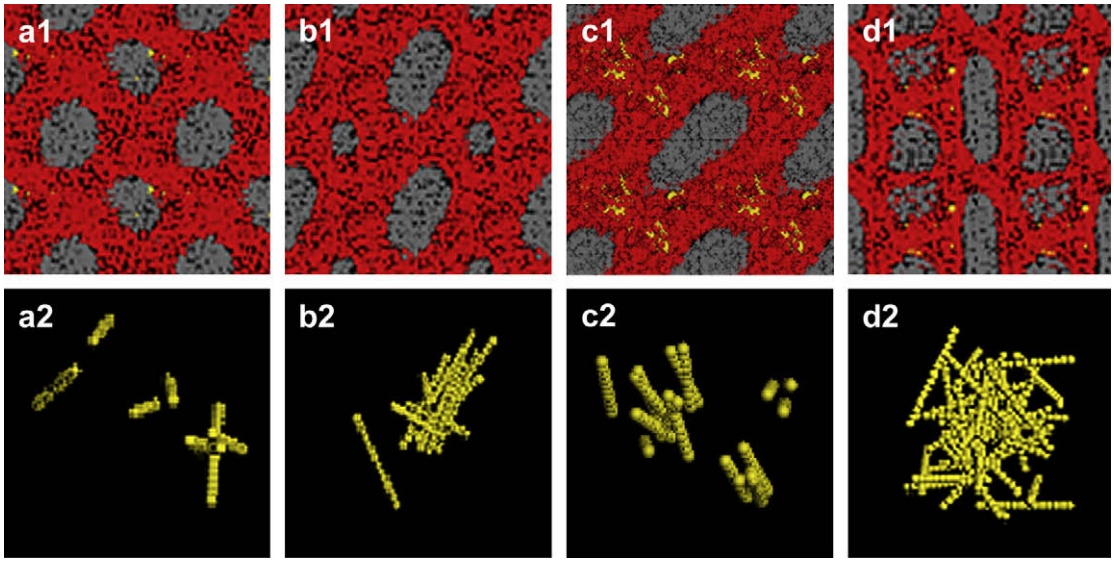

Fig. 11. Morphologies' and NRs' distributions of DBCPs' and A-attractive NRs' mixtures for $N_{rod} = 8$ (a1–a2), 12 (b1–b2), 18 (c1–c2) and 40 (d1–d2), with $L_{rod} = 3.9$.

Similarly, as shown in Fig. 9, the squares and circles respectively represent the critical NR number $N_{c\text{-}rod}$ for the mixtures transiting from cylinder (C) to ribbon (R) and from ribbon (R) to large cylindrical structure (C′). We also can draw the conclusion that the longer the NR length L_{rod} is, the stronger the effect on the final morphology is.

3.3. B-attractive nanorods

The situation for copolymer/nanorod mixtures becomes different if the NRs are preferred by the majority (B) rather than the minority (A) phase. For the length of nanorods L_{rod} is in the range of 0.3–6.9, we find that the morphological transitions of the mixtures show the same regularities as increasing N_{rod}. Take $L_{rod} = 0.3$ and $L_{rod} = 3.9$ for example, the morphologies of the mixtures and NRs' distributions are shown in Figs. 10 and 11, respectively. The both morphological transitions of the mixtures are expressed as C → R → D. With more NRs added in the fluid, in comparison with A-attractive NRs, we can see that the B-attractive NRs are mainly distributed in the favorable B domains and suffer weaker confinement from the host phase, so the NRs are not well oriented distributed in the polymer matrix, inducing the disordered structure (D).

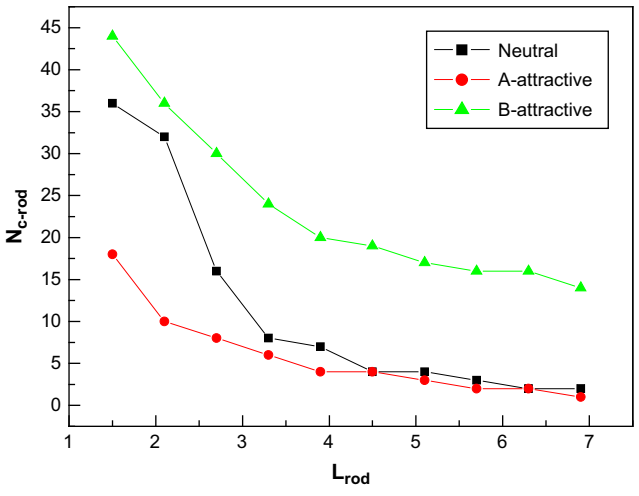

Fig. 12. The critical nanorod number $N_{c\text{-}rod}$ from cylindrical to ribbon morphologies as a function of the nanorod length L_{rod} for DBCPs and neutral, A/B attractive NRs' mixtures. Here, L_{rod} varies from 0.9 to 6.9.

Finally, we combine with the three types of NRs (neutral, A and B attractive), and present the relationship between $N_{c\text{-}rod}$ from cylinder to ribbon and L_{rod}. As shown from Fig. 12, on the one hand, it further verifies the conclusion that whether for neutral or A/B attractive NRs, the longer L_{rod} is, the stronger the effect on the final morphology is. On the other hand, for the B-attractive NRs, the values of $N_{c\text{-}rod}$ are basically higher than the other two cases. Therefore, it proves the above inference that B-attractive NRs in A_3B_7 melt have larger activity space, and more NRs are needed to give rise to the morphological transition from cylinder to ribbon.

4. Conclusions

We use the DPD method to examine the mixtures of the cylindrical DBCPs and mobile NRs. A series of parameters, such as NR number, length, and surface adsorption (neutral, A and B attractive), are introduced to analyse the cooperative phase behavior and novel morphologies of the hybrids. It is concluded that there is a consideration of enthalpic and entropic interactions when physically or chemically distinct NRs are introduced into the copolymer–nanorod composites. On the one hand, the NRs' distributions reveal a degree of enthalpically driven self-assembly, due to the attractions or repulsions among species. On the other hand, the NRs' aggregates and orientation show a degree of entropically generated self-assembly, based on the competition between the inherent shape anisotropy of NRs and confinement of host phase separated domains. For the short NRs, the stretching required by the polymers to circumvent the solid NRs is less significant, whose phase behavior of NRs is similar to that of spherical NPs. While for the long NRs under stronger confinement from the host phase, they will aggregate and self-assemble, inducing the transitions of the mixtures from one phase to another. In addition, it is also obtained that the NR length has a dramatic effect on the final morphology of the composites. In summary, the final phase structures of the mixtures result from the mutual inducement between mesophase-forming copolymers and anisotropic NRs. Our results suggest that the diblock/nanorod mixtures can yield hybrid materials with unique spatial organization and high performance.

Acknowledgments

This research was financially supported by National Natural Science Foundation of China (Nos. 20574052, 20774066, 20874094), the Outstanding Youth Fund of China (No. 20525416), Program for New Century Excellent Talents in University (NCET-05-0538) and Natural Science Foundation of Zhejiang Province (Nos. R404047). We also thank the referees for their critical reading of the manuscript and their very good ideas.

References

[1] Alexandre M, Dubois P. Mater Sci Eng Rev 2000;28:1.
[2] Balazs AC. Curr Opin Colloid Interface Sci 2000;4:443.
[3] Giannelis EP. Appl Organomet Chem 1998;12:675.
[4] Soo PP, Huang BY, Jang YI, Chiang YM, Sadoway DR, Mayes AM. J Electrochem Soc 1999;146:32.
[5] Tseng RJ, Tsai CL, Ma LP, Ouyang JY. Nat Nanotechnol 2006;1:72.
[6] Konstantatos G, Howard I, Fischer A, Hoogland S, Clifford J, Klem E, et al. Nature (London) 2004;442:180.
[7] Gas J, Poddar P, Almand J, Srinath S, Srikanth H. Adv Funct Mater 2006;16:71.
[8] Kaittanis C, Naser SA, Perez JM. Nano Lett 2007;7:380.
[9] Jaramillo TF, Baeck SH, Cuenya BR, McFarland EW. J Am Chem Soc 2003;125:7148.
[10] Peng G, Qiu F, Ginzburg VV, Jasnow D, Balazs AC. Science 2000;288:1802.
[11] Lekkerkerker HNW, Stroobants A. Nature (London) 1998;393:305.
[12] Lopes WA, Jaeger HM. Nature (London) 2001;414:735.
[13] Adams M, Dogic Z, Keller SL, Fraden S. Nature (London) 1998;393:349.
[14] Loudet JC, Barois P, Poulin P. Nature (London) 2000;407:611.
[15] Thompson RB, Ginzburg VV, Matsen MW, Balazs AC. Science 2001;292:2469.
[16] Thompson RB, Ginzburg VV, Matsen MW, Balazs AC. Macromolecules 2002;35:1060.
[17] Bockstaller MR, Thomas EL. Phys Rev Lett 2004;93:166106.
[18] Lee JY, Shou Z, Balazs AC. Phys Rev Lett 2003;91:136103.
[19] Lin Y, Böker A, He J, Sill K, Xiang H, Abetz C, et al. Nature (London) 2005;434:55.
[20] Lee JY, Thompson R, Jasnow D, Balazs AC. Macromolecules 2002;35:4855.
[21] Sun YS, Jeng US, Liang KS, Yeh SW, Wei KH. Polymer 2006;47:1101.
[22] Kim BJ, Chiu JJ, Yi GR, Pine DJ, Kramer EJ. Adv Mater 2005;17:2618.
[23] Yeh SW, Wei KH, Sun YS, Jeng US, Liang KS. Macromolecules 2005;38:6559.
[24] Bockstaller MR, Lapetnikov Y, Margel S, Thomas EL. J Am Chem Soc 2003;125:5276.
[25] Chiu JJ, Kim BJ, Kramer EJ, Pine DJ. J Am Chem Soc 2005;127:5036.
[26] Yeh SW, Chang YT, Chou CH, Wei KH. Macromol Rapid Commun 2004; 25:1679.
[27] Lee JY, Thompson RB, Jasnow D, Balazs AC. Phys Rev Lett 2002;89. 155503-1.
[28] Huh J, Ginzburg VV, Balazs AC. Macromolecules 2000;33:8085.
[29] He LL, Zhang LX, Liang HJ. J Phys Chem B 2008;112:4194.
[30] Schultz AJ, Hall CK, Genzer J. Macromolecules 2005;38:3007.
[31] de Gennes PG, Prost J. The physics of liquid crystals. Oxford: Oxford University Press; 1993.
[32] Buxton GA, Balazs AC. J Chem Phys 2002;117:7649.
[33] Huynh WU, Dittmer JJ, Alivisatos AP. Science 2002;295:2425.
[34] Laicer CST, Chastek TQ, Lodge TP, Taton TA. Macromolecules 2005;38:9749.
[35] Laicer CST, Mrozek RA, Taton TA. Polymer 2007;48:1316.
[36] Sevink GJA, Zvelindovsky AV, van Vlimmeren BAC, Maurits NM, Fraaije JGEM. J Chem Phys 1999;110:2250.
[37] He LL, Zhang LX, Liang HJ. Polymer 2009;50:721.
[38] Zhang QL, Gupta S, Emrick T, Russell TP. J Am Chem Soc 2006;128:3898.
[39] Bećneut K, Constantin D, Davidson P, Dessombz A, Chanećac C. Langmuir 2008;24:8205.
[40] Ranjan DD, Liu Y, Russell JC. Nano Lett 2007;7:3662.
[41] Balazs AC, Emrick T, Russell TP. Science 2006;314:1107.
[42] Chen K, Ma YQ. J Chem Phys 2002;116:7783.
[43] Chen K, Ma YQ. Phys Rev E 2002;65:041501.
[44] Buxton GA, Balazs AC. Mol Simul 2004;30:249.
[45] He LL, Zhang LX, Liang HJ. J Chem Phys 2009;130:144907.
[46] Hoogerbrugge PJ, Koelman JMVA. Europhys Lett 1992;19:155.
[47] Espanol P. Europhys Lett 1997;40:631.
[48] Huang CI, Chiou YJ, Lan YK. Polymer 2007;48:877.
[49] AlSunaidi BA, den Otter WK, Clarke JHR. Phil Trans R Soc Lond 2004; 362:1773.
[50] Hore MJA, Laradji MJ. Chem Phys 2008;128:054901.
[51] Hore MJA, Laradji M. J Chem Phys 2007;126:244903.
[52] Groot RD, Madden TJ. J Chem Phys 1998;108:8713.
[53] Groot RD, Warren PB. J Chem Phys 1997;107:4423.
[54] Maly M, Posocco P, Pricl S, Fermeglia M. Ind Eng Chem Res 2008;47:5023.
[55] Kim BJ, Bang J, Hawker CJ, Kramer EJ. Macromolecules 2006;39:4108.